ISSN 1063-7834, Physics of the Solid State, 2006, Vol. 48, No. 10, pp. 2021–2027. © Pleiades Publishing, Inc., 2006.
Original Russian Text © L.A. Chernozatonskiĭ, P.B. Sorokin, A.S. Fedorov, 2006, published in Fizika Tverdogo Tela, 2006, Vol. 48, No. 10, pp. 1903–1908.

FULLERENES
AND ATOMIC CLUSTERS

Energy and Electronic Properties of Non-Carbon Nanotubes Based on Silicon Dioxide

L. A. Chernozatonskiĭ[a], P. B. Sorokin[b], and A. S. Fedorov[b]

[a] *Émanuel Institute of Biochemical Physics, Russian Academy of Sciences, ul. Kosygina 4, Moscow, 119991 Russia*
e-mail: cherno@sky.chph.ras.ru

[b] *Kirensky Institute of Physics, Siberian Division, Russian Academy of Sciences, Akademgorodok, Krasnoyarsk, 660036 Russia*

Received December 20, 2005

Abstract—The geometric, energy, and electronic characteristics of new non-carbon nanotubes based on silicon dioxide are investigated in the framework of the local electron density functional formalism. Nanotubes are classified according to the type of rolling-up of the SiO_2 sheet. It is shown that, among the entire set of considered nanotubes with different symmetries, the (6, 0) nanotubes are energetically more favorable. The densities of states for nanotubes are calculated. It is established that all nanotubes are dielectrics with a wide band gap. The band gap varies over a wide range with a change in the longitudinal strain of the nanotube.

PACS numbers: 61.46.Fg, 73.63.Fg, 77.84.–s

DOI: 10.1134/S1063783406100337

1. INTRODUCTION

Since the discovery of carbon nanotubes in 1991 by Iijima [1], nanotubes have continued to attract the attention of researchers owing to their unique combination of electronic and physical properties [1]. A great variety of non-carbon nanotubes composed of different elements, for example, $(Mo,W)S_2$, BN, etc. [2], have been synthesized over the past few years. The existence of nanotubes with other compositions, such as $(Mg,Be,Zr)B_2$ diboride nanotubes [3] and BeO oxide nanotubes [4], has been predicted theoretically. This has opened up fresh opportunities for their use in electronic, optical, and electromechanical devices.

The particular interest expressed by researchers in the structures based on silicon dioxide is associated with their interesting electronic and optical properties. The best known crystalline modification of silicon dioxide is α-quartz, which is widely used in modern electronics.

In recent years, there have appeared a large number of papers concerned with hypothetical clusters [5–8] and zeolites [9] based on silicon dioxide. Many experimental works have dealt with the preparation of pseudocrystalline and amorphous nanotubes [10–12] and nanowires based on SiO_x (x = 1–2) [13]. However, the geometric structure of SiO_2 nanotubes is as yet unclear. In recent papers [14, 15], it was noted that there can exist a new class of energetically stable nanotubes composed of one SiO_2 layer with a square lattice. In [14], however, the calculations were performed using rather crude semiempirical methods. In [15], the structure was considered only for very thin nanotubes. In the present work, the geometric, energy, and electronic characteristics of a large number of single-walled SiO_2 nanotubes were investigated by the ab initio method. Moreover, we considered their possible applications as protective coatings for carbon nanotubes.

2. CLASSIFICATION OF NANOTUBES

Single-walled SiO_2 nanotubes, like dichalcogenide nanotubes [2], are formed from three cylinders: O(o) oxygen atoms lying on the outer cylinder and O(i) oxygen atoms lying on the inner cylinder with respect to the central cylinder with silicon atoms [14]. Like hexagonal nanotubes [1–3], the SiO_2 nanotubes under consideration can be constructed by hypothetically rolling up a planar structure based on a square lattice (rather than on a hexagonal lattice) formed by oxygen atoms (Fig. 1) that are tetrahedrally arranged around the silicon atoms. Therefore, SiO_2 nanotubes can be easily described in terms of two integral indices (n, m) specifying a two-dimensional developed square lattice: $\mathbf{C} = n\mathbf{a}_1 + m\mathbf{a}_2$, where the length of the chiral vector $\mathbf{C}$ is equal to the circumference of the cylindrical layer consisting of atoms. However, it should be noted that there are a number of differences between the classifications of SiO_2 and hexagonal nanotubes.

(1) The nanotubes with the indices (n, 0) and (0, n) have been referred to not as zigzag nanotubes, as is the case with hexagonal nanotubes, but as linear nanotubes (Fig. 2a) owing to their geometric structure. These nanotubes are the sole nanotubes that have no screw axes.

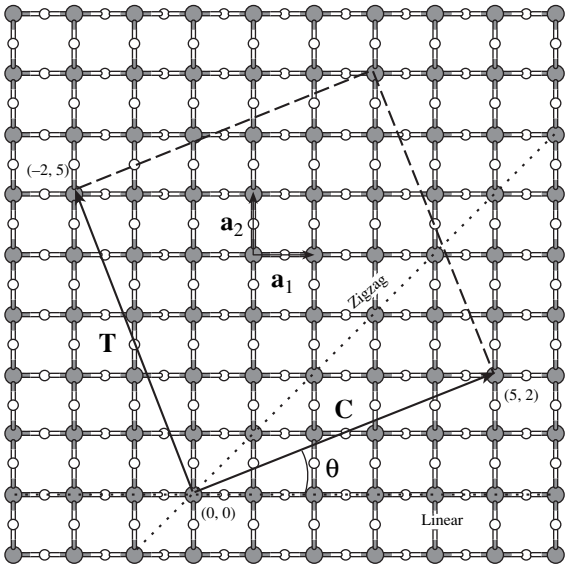

Fig. 1. Schematic drawing of the developed square lattice of a SiO_2 nanotube. Closed circles indicate silicon atoms, and open circles represent oxygen atoms. Designations: **T** is the translation vector [T = (–2, 5)], and **C** is the chiral vector [C = (5, 2)]. The oxygen atoms located along the unit vectors $\mathbf{a}_1$ and $\mathbf{a}_2$ deviate from the layer of Si atoms in upward and downward directions relative to the drawing plane, respectively.

(2) For the same reason, the (n, n) nanotubes should be referred to as zigzag nanotubes (Figs. 2b, 3a).

(3) The nanotubes with the indices (n, m) and (m, n) have different geometries because of the difference in the arrangement of the outer and inner oxygen atoms with respect to the silicon atoms located on the central cylinder.

3. COMPUTATIONAL TECHNIQUE

All the calculations were performed with the Vienna Ab Initio Simulation Package (VASP) code [16–18]. This program package makes it possible to perform ab initio calculations based on the Vanderbilt pseudopotential method and expansion in a plane-wave basis set within the framework of the local density functional formalism [20, 21]. The geometry was optimized using nine k points in the Brillouin zone along the axis of the nanotube. The k points were generated by the Monkhorst–Pack method [22]. The geometry optimization was carried out until the forces acting on each atom became less than 0.05 eV/Å.

Before calculating the nanotubes under investigation, we calculated the corresponding characteristics for a quartz crystal. The results of this preliminary calculation showed that the geometric characteristics of SiO_2 structures can be predicted with a good accuracy, namely, accurate to within 0.01 Å (compare with the experimental data taken from [23] for α-quartz: a_{calcd} = 4.913 Å and a_{exp} = 4.914 Å, c_{calcd} = 5.4049 Å and c_{exp} = 5.4054 Å). However, the band gap proved to be underestimated: E_{calcd} = 5.9 eV and E_{exp} = 8.9 eV [24]. This disadvantage of the local density functional method is well known. For this reason, the band gap of SiO_2 nanotubes can only be discussed qualitatively. In order to calculate the characteristics of a carbon nanotube cluster covered with a SiO_2 cluster, we used the PM3 semiempirical method (Parametric Model 3) included in the GAMESS program package [25].

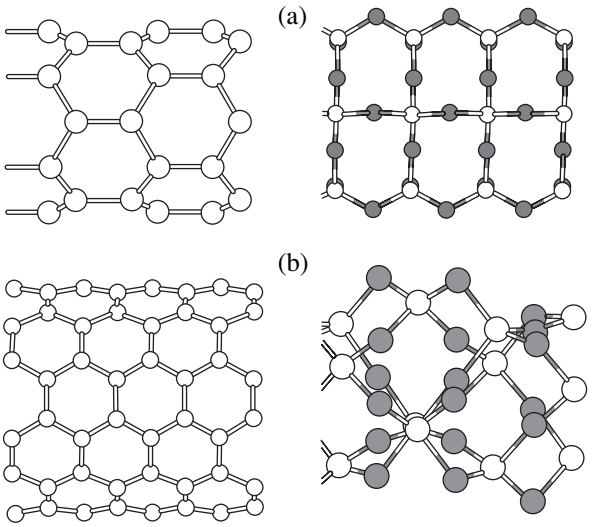

Fig. 2. Comparison of the geometric shapes of the carbon nanotubes (at the left) and the SiO_2 nanotubes (at the right): (a) the (6, 0) nanotubes and (b) the (3, 3) nanotubes.

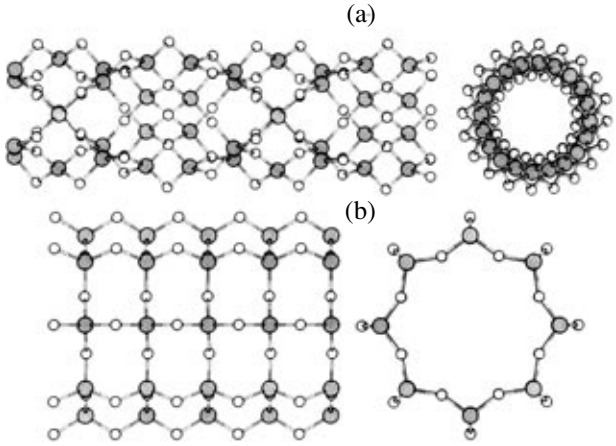

Fig. 3. Structures of (a) the (4, 4) SiO_2 zigzag nanotubes and (b) the (8, 0) SiO_2 linear nanotubes.

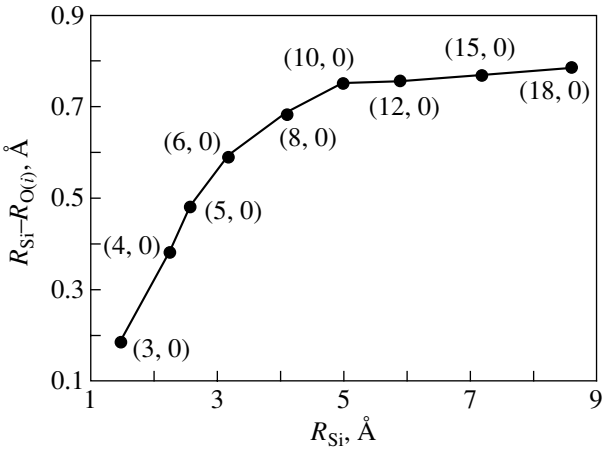

Fig. 4. Dependence of the difference between the radii of the silicon layer and the inner oxygen layer on the radius of the silicon layer for a number of SiO_2 linear nanotubes.

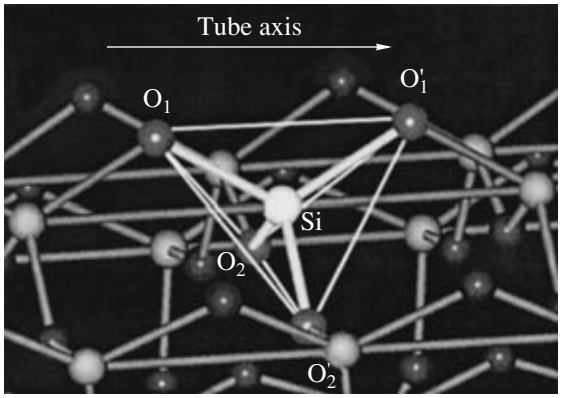

Fig. 5. Arrangement of atoms in the (n, 0) SiO_2 nanotube. The silicon atoms are located on the central nanotube cylinder. The O_1 and O_1' oxygen atoms are positioned on the outer nanotube cylinder, and the O_2 and O_2' oxygen atoms lie on the inner nanotube cylinder.

4. GEOMETRIC CHARACTERISTICS OF THE NANOTUBES

We calculated a number of (n, 0) linear nanotubes (n = 3–6, 8, 10, 12, 15, 18) and (n, n) zigzag nanotubes (n = 3, 4). As an example of SiO_2 nanotube structures, the (6, 0) and (3, 3) nanotubes are shown in Fig. 2 and the (8, 0) and (4, 4) nanotubes are depicted in Fig. 3.

The results of calculating the geometric characteristics can be summarized as follows.

The difference between the radii R of the silicon layer and the inner layer of O(i) oxygen atoms, as well as the difference between the radii R of the outer layer of O(o) oxygen atoms and the silicon layer, tends to reach the difference between the radii of the corresponding atomic layers in the planar structure (Fig. 4).

The bond lengths parallel and perpendicular to the axis of the nanotube also tend to reach the corresponding values for the planar structure (Table 1). Since the silicon atom resides in the tetrahedral environment, the bond angles in the most stable structure should be close to those in a regular tetrahedron (Fig. 5, Table 2).

It is known that atomic relaxation brings about the formation of a corrugated cylindrical surface of BN

Table 1. Main geometric characteristics of different SiO_2 nanotubes

n, m	R, Å			R_{Si}–$R_{O(i)}$, Å	$R_{O(o)}$–R_{Si}, Å	Si–O bond length, Å		Si–Si bond length, Å	
	O(i)	Si	O(o)			parallel	perpendicular	parallel	perpendicular
(3, 0)	1.31	1.50	2.24	0.18	0.74	1.65	1.63	2.82	3.00
(4, 0)	1.88	2.26	3.12	0.38	0.86	1.65	1.62	2.81	3.19
(5, 0)	2.13	2.61	3.42	0.48	0.82	1.65	1.61	2.81	3.22
(6, 0)	2.61	3.20	4.06	0.59	0.86	1.65	1.61	2.81	3.20
(8, 0)	3.44	4.12	4.98	0.68	0.86	1.65	1.62	2.83	3.15
(10, 0)	4.24	4.99	5.85	0.75	0.86	1.65	1.62	2.82	3.08
(12, 0)	5.16	5.91	6.78	0.75	0.87	1.66	1.63	2.84	3.06
(15, 0)	6.41	7.18	8.05	0.77	0.87	1.65	1.63	2.83	3.01
(18, 0)	7.82	8.61	9.48	0.78	0.87	1.66	1.63	2.84	2.98
(3, 3)	1.59	2.02	2.92	0.44	0.90	1.68	1.64	2.65	2.64
(4, 4)	2.03	2.64	3.51	0.61	0.88	1.68	1.63	2.67	2.68
(0, 10)	3.85	4.56	5.33	0.71	0.78	1.64	1.72	2.95	3.27
Planar structure				0.87	0.87	1.65	1.63	2.78	2.79

Note: The bond lengths were calculated in different (parallel and perpendicular) directions with respect to the axis of the SiO_2 nanotube.

Table 2. Angles between atoms in different SiO_2 nanotubes (the designations of the atoms correspond to those used in Fig. 5)

n, m	Angle, deg			Δ, deg		
	O_1–Si–O'_1	O_2–Si–O'_2	O_1–Si–O'_2			
(3, 0)	118.132	106.959	107.314	8.66	2.51	2.16
(4, 0)	116.88	109.79	107.77	7.41	0.31	1.71
(5, 0)	117.24	109.27	107.38	7.77	0.20	2.09
(6, 0)	117.20	108.74	107.89	7.73	0.73	1.58
(8, 0)	117.54	108.45	107.77	8.07	1.02	1.70
(10, 0)	117.31	108.98	107.78	7.84	0.49	1.69
(12, 0)	117.81	109.99	107.14	8.34	0.51	2.33
(15, 0)	117.39	111.11	107.09	7.92	1.64	2.38
(18, 0)	118.14	110.61	106.99	8.67	1.13	2.49
(3, 3)	132.96	123.05	102.32	23.49	13.58	7.15
(4, 4)	129.97	118.63	105.52	20.49	9.16	3.95
(0, 10)	128.07	143.66	39.69	18.60	34.19	69.78
Planar structure	116.29	116.25	105.68	6.82	6.78	3.79

nanotubes [26]. In turn, this leads to the formation of an energetically more favorable configuration. A similar effect regarding an energetically more favorable configuration also manifests itself for SiO_2 nanotubes: the SiO_2 layer fragment, unlike the graphite layer fragment, has an optimum "saddle" shape rather than a planar shape [14].

5. ENERGY CHARACTERISTICS OF THE NANOTUBES

The energy of a number of SiO_2 linear nanotubes was calculated as a function of the silicon layer radius. It can be seen from Fig. 6 that the (6, 0) SiO_2 nanotube is energetically more favorable. This result can be explained by the fact that the geometric configuration of the tetrahedral environment of the silicon atoms in this structure is most similar to a regular unstrained configuration. The calculation of the (3, 3) and (4, 4) SiO_2 zigzag nanotubes has demonstrated that these structures are energetically less favorable (E = –22.42 and –22.55 eV/SiO_2, respectively) than the (n, 0) linear nanotubes with a close diameter (E = –23.43 eV/SiO_2 for the (10, 0) nanotube). Furthermore, the absolute value of the calculated energy of the (0, 10) nanotube (E = –21.58 eV/SiO_2) turned out to be less than that of

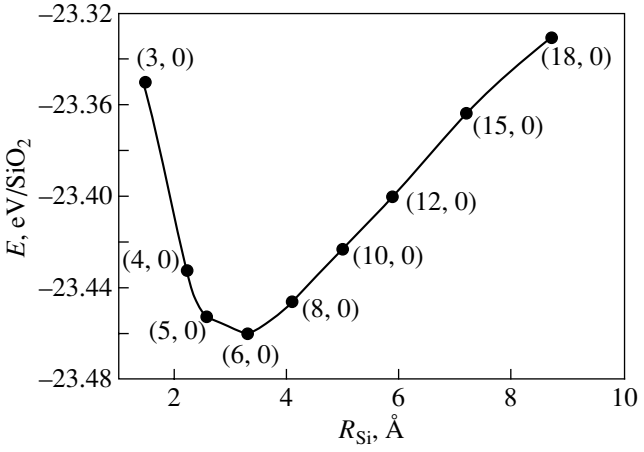

Fig. 6. Dependence of the energy of the linear nanotubes per SiO_2 molecule on the radius of the layer formed by silicon atoms.

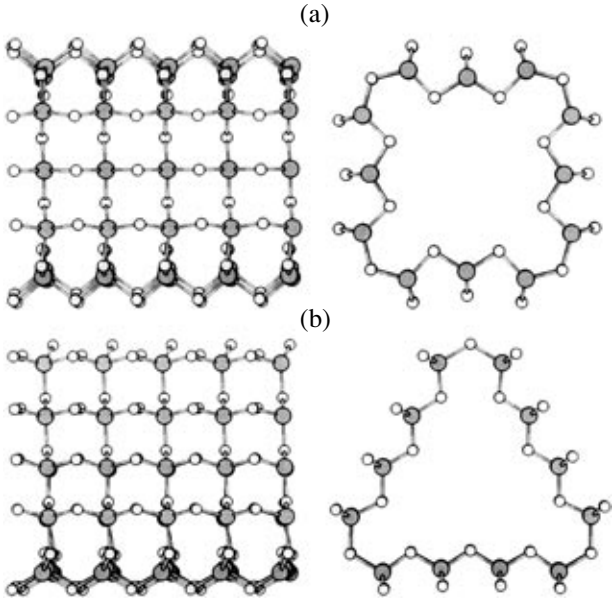

Fig. 7. (a) SiO_2 square nanotubes and (b) SiO_2 triangular nanotubes.

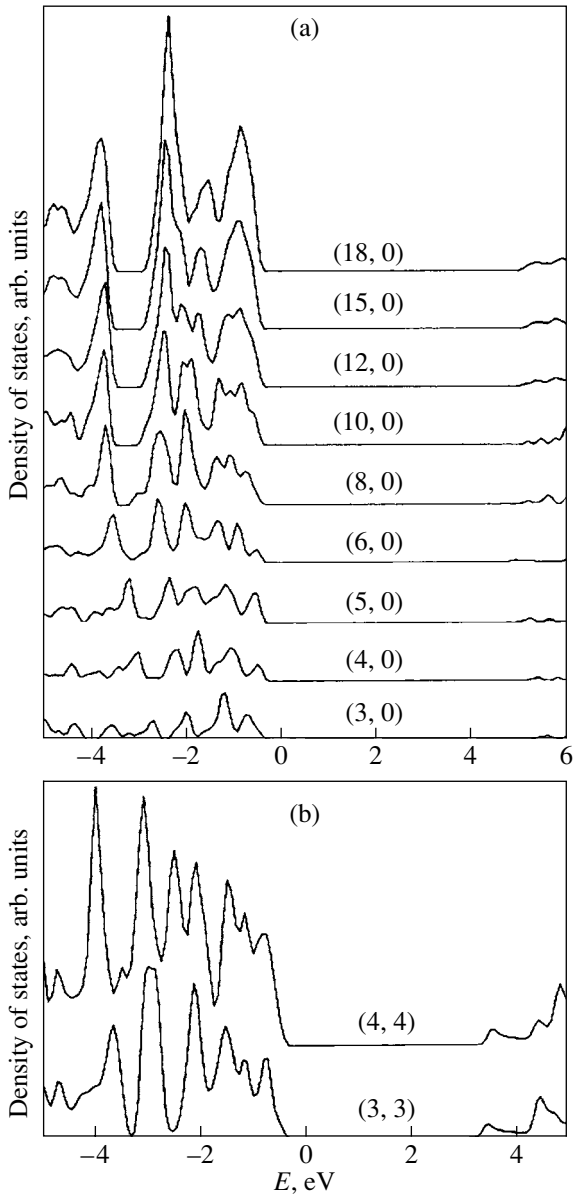

Fig. 8. Densities of states for (a) the linear nanotubes and (b) the zigzag nanotubes.

the (10, 0) nanotube. Therefore, we can conclude that the synthesis will most likely result in the formation of (n, 0) linear nanotubes.

In addition to the above structures, we considered SiO_2 nanotubes composed of ten "lines" of silicon atoms with square (Fig. 7a) and triangular (Fig. 7b) cross sections formed by oxygen atoms. The initial energies of these nanotubes are equal to –21.6 and –21.8 eV/SiO_2, respectively. After the energy optimization, these structures take on a standard circular shape characteristic of (10, 0) nanotubes. Despite this result, it can be assumed that similar noncircular structures are formed in bundles of SiO_2 nanotubes owing to the high flexibility of Si–O–Si bonds.

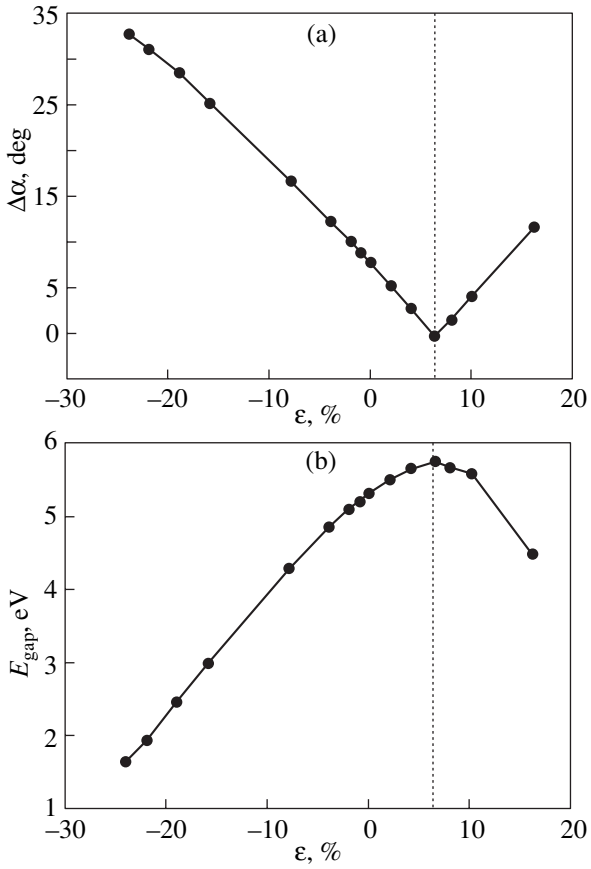

Fig. 9. Dependences of (a) the difference between the O_1–Si–O_1' bond angle and the bond angle of 109.471° formed by the oxygen atoms in the SiO_4 tetrahedron and (b) the band gap on the strain of the SiO_2 nanotubes.

6. ELECTRONIC BAND STRUCTURE AND ITS DEPENDENCE ON THE STRAIN OF THE NANOTUBE

The results of our calculations have demonstrated that the nanotubes under investigation are dielectrics with a wide band gap. As the nanotube radius increases, the band gap tends to reach the corresponding value for the planar structure. The densities of states for the linear and zigzag nanotubes are shown in Figs. 8a and 8b, respectively. It can be seen from these figures that, as the transverse size of the nanotubes increases, the band gap decreases in the linear nanotubes and increases in the zigzag nanotubes.

It is known [27] that deformation of nanotubes based on boron nitride leads to a change in the band gap. In order to verify this effect for SiO_2 nanotubes, we analyzed the change in the electronic band structure of the energetically most stable (6, 0) SiO_2 nanotube. Figure 9 depicts the calculated dependence of the difference $\Delta\alpha$ between the largest O–Si–O bond angle in the nanotube structure and the corresponding angle in the quartz structure (Fig. 9a) and the dependence of the

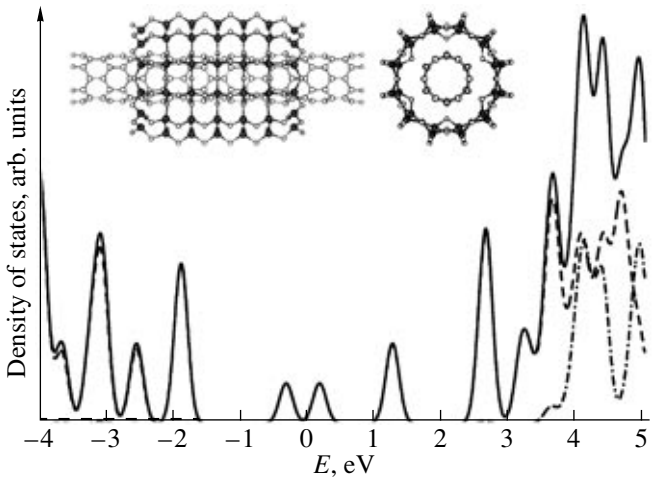

Fig. 10. Densities of states for nanotubes. The solid line indicates the density of states for a system consisting of the (6, 0) carbon nanotube fragment inserted into the (12, 0) SiO_2 nanotube fragment. The dashed and dot-dashed lines represent the densities of states for the (6, 0) carbon nanotube and the (12, 0) SiO_2 nanotube, respectively. The inset shows the structure of "(6, 0) carbon nanotube–(12, 0)@SiO_2 nanotube" clusters.

band gap (Fig. 9b) on the longitudinal strain $\varepsilon = \frac{l_0 - l}{l_0} \times 100\%$ for the (6, 0) SiO_2 nanotube (where l_0 and l are the lengths of the initial unstrained and strained unit cells of the nanotube, respectively). As can be seen from Fig. 9b, the band gap in the electronic spectrum of the SiO_2 nanotube depends substantially on the longitudinal strain. It should be noted that the band gap reaches a maximum for the strain at which the O–Si–O bond angle under compression of the nanotube becomes equal to the corresponding angle in the quartz structure ($\Delta\alpha = 0$); i.e., in the case where the atomic configuration of the nanotube most closely resembles the atomic configuration of the quartz structure. Therefore, the deformation of SiO_2 nanotubes should affect their electronic properties.

7. FIELD OF APPLICATION OF THE NANOTUBES

Owing to the screw axis ($n \neq 0, m \neq 0$), the SiO_2 nanotubes should possess piezoelectric properties, as is the case with BN nanotubes [28] and quartz crystals. The silicon dioxide nanotubes under consideration can be used as materials for fabricating springs and mechanoelectrical elements in micromachines, as building blocks for the design of new nanomaterials, and as objects for protecting carbon nanotubes against external actions, because SiO_2 nanotubes with fully saturated atomic bonds are chemically inert insulating materials. The idea of creating such protection is not new. In particular, Golberg et al. [29] synthesized BN nanotubes on carbon nanotubes. Enyashin et al. [30] theoretically proved that a dielectric single-walled BN nanotube insulates a conducting carbon nanotube. In recent years, a large number of experimental works have dealt with the deposition of SiO_2 amorphous layers onto carbon nanotubes [31, 32]. In this study, the interaction between the SiO_2 and carbon nanotubes was calculated using the PM3 semiempirical method. We considered a cluster system consisting of a (6, 0) carbon nanotube fragment ($C_{228}H_{12}$ cluster) inserted into a (12, 0) SiO_2 nanotube fragment (see the inset to Fig. 10). The geometry optimization has established that the final configuration is stable and remains virtually unchanged as compared to the initial structures. The analysis of the density of states (Fig. 10) has demonstrated that the SiO_2 nanotube does not substantially contribute to the region in the vicinity of the Fermi energy. Therefore, the electronic structure of the SiO_2 nanotube has no effect on the conductivity of the protected carbon nanotube.

8. CONCLUSIONS

Thus, the geometric, energy, and electronic characteristics of new non-carbon nanotubes based on a SiO_2 square lattice were investigated in the framework of the local electron density functional formalism. We examined nanotubes of different types. It was demonstrated that linear nanotubes are energetically more favorable and that the (6, 0) SiO_2 nanotube has the lowest energy. The densities of states for the SiO_2 nanotubes were calculated. It was revealed that all nanotubes are dielectrics with a wide band gap. The band gap of the nanotubes was shown to vary over a wide range depending on the longitudinal strain. The possibility of fabricating a protective coating from a SiO_2 nanotube for a carbon nanotube was analyzed.

ACKNOWLEDGMENTS

We would like to thank the Institute of Computer Modeling (Siberian Division, Russian Academy of Sciences, Russia) and the Joint Supercomputer Center of the Russian Academy of Sciences for providing an opportunity to use cluster computers for performing the quantum-chemical calculations.

This work was supported by the Russian Foundation for Basic Research (project no. 05-02-17443) and Deutsche Forschungsgemeinschaft (project no. 436 RUS 113/785).

REFERENCES

1. J. Charlier and S. Iijima, in *Topics in Applied Physics*, Vol. 80: *Carbon Nanotubes: Synthesis, Structure, Properties, and Applications*, Ed. by M. S. Dresselhaus, G. Dresselhaus, and Ph. Avouris (Springer, Berlin, 2001), p. 81.

2. R. Tenne and A. K. Zettl, in *Topics in Applied Physics*, Vol. 80: *Carbon Nanotubes: Synthesis, Structure, Properties, and Applications*, Ed. by M. S. Dresselhaus, G. Dresselhaus, and Ph. Avouris (Springer, Berlin, 2001), p. 55.
3. L. A. Chernozatonskiĭ, Pis'ma Zh. Éksp. Teor. Fiz. **74** (6), 369 (2001) [Phys. Solid State **74** (6), 335 (2001)].
4. P. B. Sorokin, A. S. Fedorov, and L. A. Chernozatonskiĭ, Fiz. Tverd. Tela (St. Petersburg) **48** (2), 373 (2006) [Phys. Solid State **48** (2), 398 (2006)].
5. M. A. Zwijnenburg, S. T. Bromley, E. Flikkema, and T. Maschmeyer, Chem. Phys. Lett. **385**, 389 (2004).
6. S. T. Bromley, M. A. Zwijnenburg, and Th. Maschmeyer, Phys. Rev. Lett. **90**, 035502 (2003).
7. J. Song and M. Choi, Phys. Rev. B: Condens. Matter **65**, 241302 (2002).
8. M. W. Zhao, R. Q. Zhang, and S. T. Lee, Phys. Rev. B: Condens. Matter **70**, 205404 (2004).
9. M. A. Zwijnenburg, S. T. Bromley, J. C. Jansen, and T. Maschmeyer, Chem. Mater. **16**, 12 (2004).
10. M. Adachi, Colloid Polym. Sci. **281**, 370 (2003).
11. M. Zhang, E. Ciocan, Y. Bando, K. Wada, L. L. Cheng, and P. Pirouz, Appl. Phys. Lett. **80**, 491 (2002).
12. Y. Li, Y. Bando, and D. Goldberg, Adv. Mater. **16**, 37 (2004).
13. N. I. Kovtyukova, T. E. Mallouk, and T. S. Mayer, Adv. Mater. **15**, 780 (2003).
14. L. A. Chernozatonskiĭ, Pis'ma Zh. Éksp. Teor. Fiz. **80** (10), 732 (2004) [JETP Lett. **80** (10), 628 (2004)].
15. A. K. Singh, V. Kumar, and Y. Kawazoe, Phys. Rev. B: Condens. Matter **72**, 155422 (2005).
16. G. Kresse and J. Hafner, Phys. Rev. B: Condens. Matter **47**, 558 (1993).
17. G. Kresse and J. Hafner, Phys. Rev. B: Condens. Matter **49**, 14251 (1994).
18. G. Kresse and J. Furthmüller, Phys. Rev. B: Condens. Matter **54**, 11169 (1996).
19. D. Vanderbilt, Phys. Rev. B: Condens. Matter **41**, 7892 (1990).
20. P. Hohenberg and W. Kohn, Phys. Rev. **136**, 864 (1964).
21. W. Kohn and L. J. Sham, Phys. Rev. **140**, 1133 (1965).
22. H. J. Monkhorst and J. D. Pack, Phys. Rev. B: Solid State **13**, 5188 (1976).
23. A. A. Blistanov, V. S. Bondarenko, N. V. Perelomova F. N. Strizhevskaya, and V. V. Chkalova, *A Handbook on Acoustic Crystals*, Ed. by M. P. Shaskol'skaya (Nauka, Moscow, 1982) [in Russian].
24. R. B. Laughlin, Phys. Rev. B: Condens. Matter **22**, 3021 (1980).
25. M. W. Schmidt, K. K. Baldridge, J. A. Boatz, S. T. Elbert, M. S. Gordon, J. H. Jensen, S. Koseki, N. Matsunaga, K. A. Nguyen, S. Su, T. L. Windus, M. Dupuis, and J. A. Montgomery, Jr., J. Comput. Chem. **14**, 1347 (1993).
26. M. Menon and D. Srivastava, Chem. Phys. Lett. **307**, 407 (1997).
27. Yong-Hyum Kim, K. J. Chang, and S. G. Louie, Phys. Rev. B: Condens. Matter **63**, 205408 (2001).
28. S. M. Nakhmanson, A. Calzolari, V. Meunier, J. Bernholc, and M. Buongiorno Nardelli, Phys. Rev. B: Condens. Matter **67**, 235406 (2003).
29. D. Golberg, W. Han, Y. Bando, L. Bourgeois, K. Kurashima, and T. Sato, J. Appl. Phys. **86**, 23649 (1999).
30. A. N. Enyashin, G. Zeĭfert, and A. L. Ivanovskiĭ, Pis'ma Zh. Éksp. Teor. Fiz. **80** (9), 709 (2004) [JETP Lett. **80** (9), 608 (2004)].
31. T. Seeger, Ph. Redlich, N. Grobert, M. Terrones, D. R. M. Walton, H. W. Krotom, and M. Rühle, Chem. Phys. Lett. **339**, 41 (2001).
32. R. Colorado, Jr. and A. R. Barron, Chem. Mater. **16**, 2691 (2004).

Translated by O. Borovik-Romanova